Wake Interference in Aeroelastic Wind Power Generation

Michael E. Isenberg, Ephrahim Garcia, Ph.D.
Cornell University

Keywords: *Aeroelastic, Flutter, Piezoelectric, Wake Interference, Power*

Abstract

This paper discusses the effects of wake interference on the power output of a small-scale flapping wind-energy harvester. The device itself is similar to a cantilevered beam, with piezoelectrics connected to the sides of the beam at the fixed end, generating a current when they are flexed. An airfoil is connected to the free end of the beam by a flexible joint, causing the device to 'flap' back and forth, similar to a fish tail. Subjected to a wind flow of a critical speed, flutter instabilities cause the airfoil to oscillate with coupled pitching and heaving vibrations. Vibrations grow in amplitude until nonlinearities in the system establish a stable limit cycle. When multiple devices are used together in a formation, the disturbance of the flow by the leading device affects the output of downstream devices depending on position.

Optimal formation layout for maximum power generation is investigated through the use of wind tunnel experimentation. Varying the stream-wise and cross-stream distances between two devices, the relationship between the position and output voltage of the trailing device is determined. Data analysis includes effects of wake interference on formation power and device stability.

1 Introduction

This paper will investigate the phenomenon of aeroelastic flutter for the application of power generation. The concept of energy harvesting using piezoelectrics to this point has focused on vibrations in host structures [1]. More recently, research has been conducted in piezoelectric „œels' attached to the downstream end of bluff bodies, utilizing the trailing vortices from these bodies to wave in the airflow [2]. The argument for this research has been the operation of small electronic devices that would otherwise require batteries that would eventually need replacing.

Traditionally, the destructive power of aeroelastic flutter is a primary concern of aircraft designers. Torsional deformation in a flow causes a pitching motion of the wing, while bending deformation creates an additional plunging motion. Flutter is a result of the coupling of these two structural modes, now denoted as modal convergence flutter. Below a certain wind speed, these oscillatory motions are dampened out by the forces of the airflow. However, above a critical flutter speed, the airflow begins to act as a negative damper and the vibrations grow exponentially. At this speed, the natural frequencies of the two modes converge and the amplitude of the oscillations grows as a result. Eventually, a steady limit cycle for the deflections is established due to nonlinearities in the system [3].

The following investigations make use of a cantilevered beam with an airfoil attached to the free end. Flutter is induced in these experiments through mass imbalance around the axis of rotation of the airfoil. With the airfoil coupled to the beam, a bending moment is created around the fixed edge of the beam. To harness energy from this motion, piezoelectrics are attached to the beam.

While the fluttering phenomenon is interesting enough to investigate on its own, a single harvester would be of little consequence in terms of providing any significant amount of power. Getting sufficient power will require arrays or formations of several devices, similar

in concept, but not in size, to much larger wind farms. Therefore, experiments led to investigating what effect the wake of an upstream harvester would have on a trailing harvester in various formations. Tests were conducted with two different models of energy harvester, one horizontal and one vertical configuration. Two harvesters were built for each configuration and each configuration was tested independently of the other. Moving the trailing harvester to various stream-wise and cross-stream separations with respect to the leading harvester, the V_{rms}, V_{p2p}, and f were recorded for both harvesters at each position. The average power through a resistive load was measured for each configuration using this data.

2 Principal Investigations

The viability of using flutter for power harvesting had already been proven [4] before the formation investigations were undertaken; therefore, these experiments focus more on the interactions between multiple fluttering devices. The motion of the harvesting devices is similar to the "flapping" motion of birds' wings [5] in flight or a fish's tail [6] while swimming. It can, therefore, be reasonably assumed that some form of wake and trailing vortices will form downstream of a harvester in airflow. The wake and trailing vortices from these harvesting devices have the potential to significantly interfere, either constructively or destructively, with the power output of a trailing harvester. By reducing the flow that eventually reaches a trailing harvester, the lift and drag forces on that airfoil are reduced and the amplitude of oscillation of the beam is reduced. The less the beam deflects, the smaller the voltage that is applied across the piezoelectric. Interference from the leading harvester can also cause irregularities in the motion of the trailing harvester. In addition to changing the amplitude, it has the potential to alter the frequency of oscillation, as well as make the flutter of the second harvester completely erratic.

The overall purpose of these experiments was to identify the optimal array configuration for multiple energy harvesters. By examining the interactions between the harvesters at the various different positions, the most beneficial position for power generation from the rear harvester could be determined. The data obtained from these experiments can then be expanded to larger arrays, with many more than two harvesters. After conducting experiments solely with the horizontal harvester, it was determined that the distance between the two airfoils should be shortened in order to better understand the interaction between them. This led to the creation of the vertical harvester and the additional experimentation.

3 Harvesting Device Design

Two different power harvesting designs were put through experimental tests. Both take the form of a cantilevered beam with an airfoil attached to the free end in order to create a deflection. The beam itself is made of stainless steel, measuring 0.381 mm thick and 25 mm wide. Using 301 stainless steel for the beam material ensured long fatigue life and aversion to yielding, as well as allowing different types of loadings.

Piezoelectric materials are materials that generate a voltage when they are deformed. The most widely used piezoelectric materials are ceramic wafers, with QP10n Transducers from MIDE used in these experiments. These transducers are easily attached to the sides of the steel beam using adhesive. In order to generate the largest voltage across the piezoelectrics, they need to be placed where they will experience maximum compression and tension. On a cantilevered beam, this criterion requires that the piezoelectrics be placed near the fixed end. Two transducers are used for each beam, with one attached to either side of the beam near the fixed end. They are then connected in parallel to combine their voltage for power generation.

Previous experimentation had determined that the shape of the airfoil did not significantly change the power output from the devices as long as the airfoils are of the same mass [7]. Hence, a simple rectangular balsa wood plate was used for these experiments. The airfoil was connected to the beam through a 3.175 mm

diameter carbon fiber tube with two ball bearings allowing rotation with minimal friction.

There are several key differences between the two harvesters, which are outlined below in Tables 1.

Component	Horizontal Harvester Dimensions	Vertical Harvester Dimensions
Beam (length from clamp to free end)	243 mm	196 mm
Shaft (length)	70 mm	140 mm
Airfoil	59 x 136 x 1.42 mm	59.5 x 136 x 2.08 mm

Table 1. Harvester Component Dimensions

Table 1 shows that the beam of the horizontal harvester is longer, while the carbon fiber shaft of the vertical harvester is longer. It is also important to note that while the width and length of the airfoils are nearly identical, the thickness of the vertical harvester wing is slightly larger.

3.1 Horizontal Harvester

The shaft is press-fit into a slot in the airfoil, with Scotch tape providing additional stability. Plastic weights attached to the top and bottom tips of the airfoil add mass to the system to increase the inertia. Ball bearings are inserted into a plastic clasp connecting the airfoil assembly and the beam. The shaft collars prevent vertical movement of the airfoil.

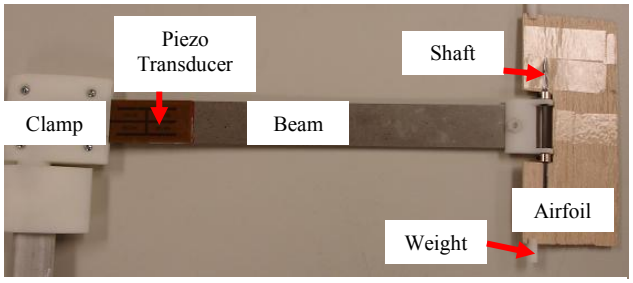

Fig. 1. Horizontal Harvester

3.2 Vertical Harvester

The vertical harvester design is seen in Fig. 2. The airfoil assembly is essentially the same as before, with ball bearings in the clasp allowing the shaft to rotate freely and shaft collars preventing vertical motion of the airfoil. For this harvester, however, the shaft is press-fit into the airfoil with modeling glue used for adhesive.

The length of the beam was determined for this model using the constraint that the first bending frequency of the two harvester designs should be the same.

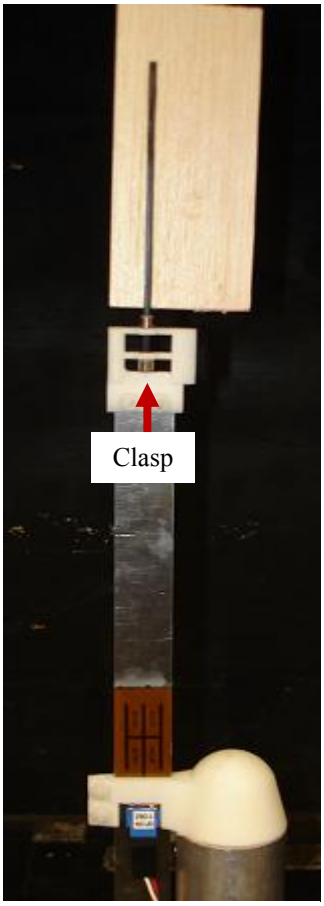

Fig. 2. Vertical Harvester

3.3 Harvester Design Differences

Table 2 outlines some important characteristics of the harvesters made for each design. The harvester masses are the masses of the wing assemblies, which exclude the masses of the beams, transducers, and clamps. The inertias of the rotating components were measured using computer-aided design in Solid Works.

	Horizontal Harvester	Vertical Harvester
Leading Harvester Mass	9.451 g	10.3243 g
Trailing Harvester Mass	8.8856 g	10.3681 g
Inertia (rotating components)	1700 g · mm^2	847.455 g · mm^2
First Bending Frequency	3.68 Hz	3.65 Hz

Table 2. Harvester Performance Characteristics

4 Experimental Equipment and Methods

4.1 Equipment

Testing was conducted in a low-speed wind tunnel, with a test section measuring 1.2 m wide x 1 m high, with six variable speed fans at the end of the tunnel, each producing flows of up to approximately 5 m/s. Measurements of frequency (f), root-mean-squared voltage (V_{rms}), and peak-to-peak voltage (V_{p2p}) were taken using an Agilent 54622A oscilloscope, which has a maximum sampling rate of 200 MSa/s per channel. Several resistors on simple circuit boards were used to create separate resistive loads for each harvester. The wind speed in the center of the tunnel was measured through the use of a hot-wire anemometer from OMEGA Technologies Company.

The harvesters in each set of experiments were elevated to near the center of the tunnel, using a pair of stings, in order to avoid boundary layer interference from either the floor or ceiling. For the horizontal harvesters, a cylindrical steel tube measuring 30.3 cm tall was mounted to a 1.27 cm thick flat plat on the floor of the tunnel. On top of this cylinder, another tear-drop shaped tube brought the total height to 55.9 cm. While the sting for the leading harvester was mounted to the center of its plate, the sting for the trailing harvester was mounted to a second flat plate with slots and rails, allowing two-degrees of translation. The second plate was also 1.27 cm thick, with the rails measuring 3.81 cm tall and the cylindrical tube 30.3 cm tall. The additional tear-drop tube and attachments made up the difference so that the trailing harvester was also at 55.9 cm above the floor.

Experiments with the vertical harvesters made use of a simpler mounting system, only utilizing the flat plate with slots and rails. In these experiments, the tear-drop tube was removed, with the actual beam of the harvester replacing this length. The leading harvester was mounted in a static position on the plate, while the trailing harvester was again mounted on the rails to allow two-degrees of translation. The airfoils in this case were elevated a total of 57.6 cm off the floor of the tunnel.

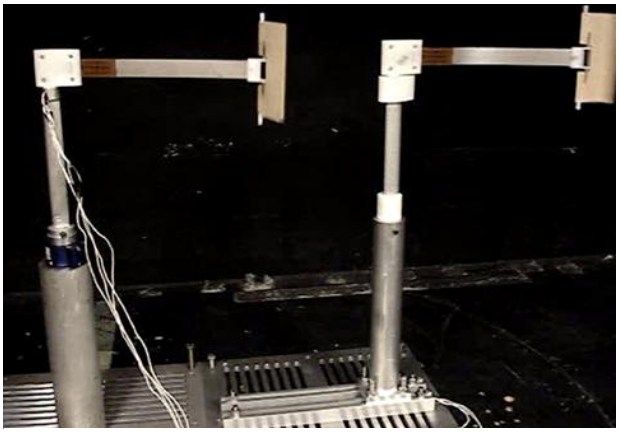

Fig. 3. Horizontal Harvester Lab Set-Up

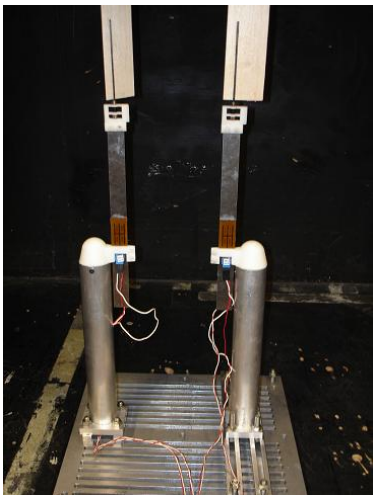

Fig. 4. Vertical Harvester Lab Set-Up

4.2 Methodology

Experimentation with multiple harvesters began with testing of the horizontal configuration. As previously stated, a significant amount of data had already been collected on the performance of a single harvester before this new study began. From those previous experiments, it had been determined that the wind speed for maximum power generation was between 7.7-7.8 m/s. The fans were adjusted accordingly, with the hotwire anemometer providing the wind speed in the test section of the tunnel. To get the largest power output (Eq. 1) from each harvester, the optimal resistive load first had to be determined. Each of the harvesters was placed alone in the tunnel and the steady-state flutter frequency was measured using the oscilloscope. This frequency reading provided an initial guess for the equivalent impedance using Eq. 2:

$$P = V_{rms}^2 / R \quad (1)$$

$$R = Z_{eq} = 1/(2 \cdot \pi \cdot f \cdot C) \quad (2)$$

The capacitance and steady-state frequencies of both horizontal harvesters were measured in order to provide an initial guess for the resistances. Using two 100 kΩ resistors and a variable resistor for each circuit, the resistances were varied by steps of 15 kΩ for each harvester, measuring V_{rms} on the oscilloscope and calculating the corresponding power from Eq. 1. Four resistances were tested for both harvesters until an optimal resistance for peak power output was found.

A similar procedure was used to determine the resistances for the vertical harvester configuration, though the wind speed in the tunnel was instead held to 4.5-4.6 m/s. While the ideal wind speed for the vertical design had not yet been determined at the time of testing, the interaction between two harvesters was the focus of the study and this wind speed was chosen for pure simplicity of testing. Also, visual observation at speeds of 7.7-7.8 m/s showed that there was significant instability, removing such speeds from consideration for power generation.

Table 3 below provides values for the properties mentioned above for both the leading and trailing harvesters in each configuration. The final resistances were used in all subsequent experimentation.

	Horizontal Harvester	Vertical Harvester
Capacitance (Leading Harvester)	116 nF	114.8 nF
Capacitance (Trailing Harvester)	116 nF	117.7 nF
Frequency (Leading Harvester)	4.66 Hz	5.36 Hz
Frequency (Trailing Harvester)	4.95 Hz	5.39 Hz
Initial Resistance (Leading Harvester)	294.4 kΩ	258.65 kΩ
Initial Resistance (Trailing Harvester)	277.2 kΩ	250.87 kΩ
Final Resistance (Leading Harvester)	250 kΩ	250 kΩ
Final Resistance (Trailing Harvester)	263 kΩ	248 kΩ

Table 3. Steady-State Frequencies and Resistive Loads

The methods for taking readings from the oscilloscope are described hence. The fans were adjusted to give the appropriate wind speeds for each configuration as outlined above. Once turned on, 30 seconds lapsed before any readings were taken in order to allow the flow to reach steady-state. Readings of f, V_{rms}, and V_{p2p} were then recorded after pressing the „SINGLE' button on the oscilloscope, which takes a snapshot of the response over a certain amount of time. The time range of the oscilloscope was adjusted to give approximately 3-4 cycles of the response, corresponding to 400,000 samples when a single harvester was tested and 200,000 samples per harvester with two channels connected. The oscilloscope then provided the averages of f, V_{rms}, and V_{p2p} over this span. After recording the necessary values, the „RUN' button on the oscilloscope was pressed so that the display was once again providing current values. An additional 15 seconds was allowed to lapse before the subsequent press of the „SINGLE' button for an additional reading. During the time between readings, the wind speed measured by the anemometer was visually studied and then an approximate value was recorded for the 15 second period.

The steady-state performance for each individual harvester was determined by placing it alone in the wind tunnel at the appropriate wind speed. Then ten readings were taken as described above and averaged. For the horizontal configuration, readings were taken at x values of 0.5, 5, 10, and 15 inches. These separations were chosen on the basis of time constraints for testing and size of the wind tunnel's testing chamber. These stream-wise separations were measured from the trailing edge of the leading harvester to the leading edge of the trailing harvester's clamp. At each x value, readings were taken at y values ranging from 0 to 15 inches at one inch intervals. Ten readings were taken at each combination of x and y and averaged to give a data point. A similar procedure was used for the vertical configuration, though the distances of stream-wise separation was measured in chord lengths in this case, from the trailing edge of the leading airfoil to the leading edge of the trailing airfoil. Values of x tested included 0.25, 1, 2, 3, and 4

chord lengths, while cross-stream *y* values ranged from 0-4 inches at one inch intervals. Again, ten readings were taken at each position and averaged to give a data point. The test set-ups for the horizontal and vertical harvesters is shown below in Figures 5 and 6.

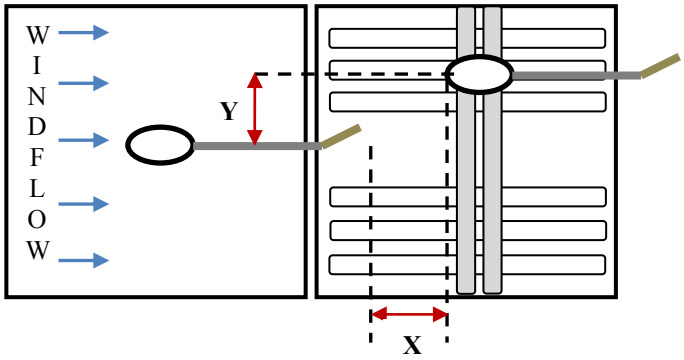

Fig. 5. Top View of Horizontal Harvester Test Set-Up

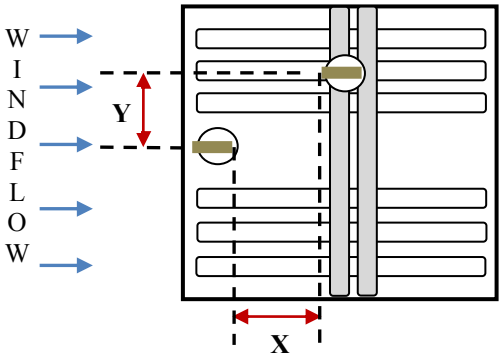

Fig. 6. Top View of Vertical Harvester Test Set-Up

5 Results

5.1 Horizontal Harvester Data

The data from the wind tunnel experiments with the horizontal harvester configuration can be seen below in Figures 7 through 10. Each individual color line represents a different stream-wise separation between the harvesters, with the plots being a function of the cross-stream separation, measured in inches. Each data point is the average of ten readings at that position, as described in the previous section. Figures 7 and 8 plot the stead-state frequency of the leading and trailing harvesters, respectively, while Figures 9 and 10 plot the power produced by the

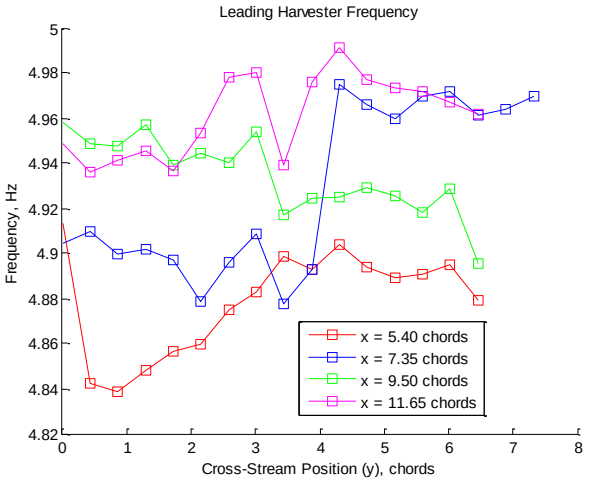

Fig. 7. Leading Horizontal Harvester Frequency

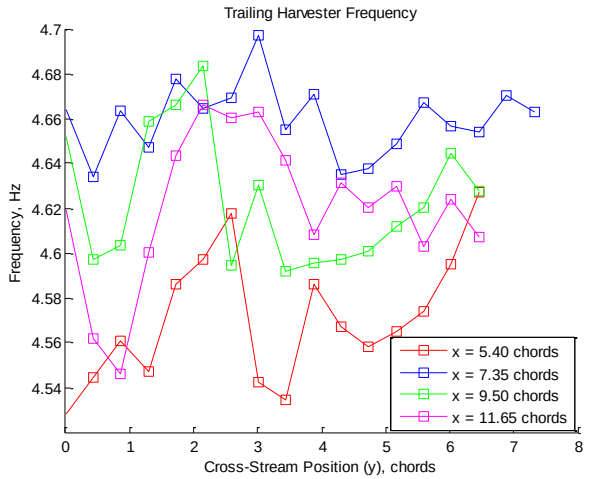

Fig. 8. Trailing Horizontal Harvester Frequency

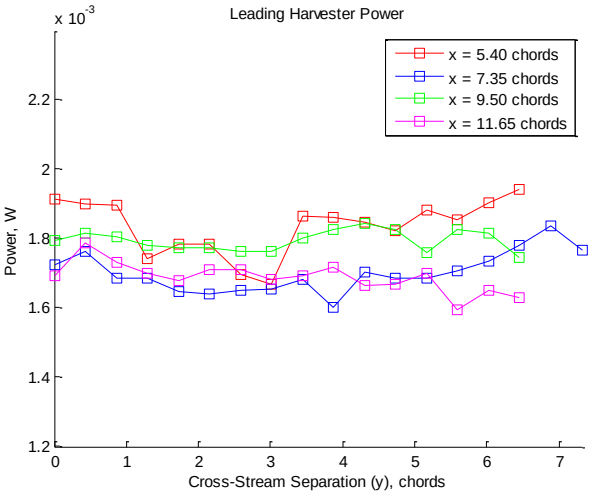

Fig. 9. Leading Horizontal Harvester Power

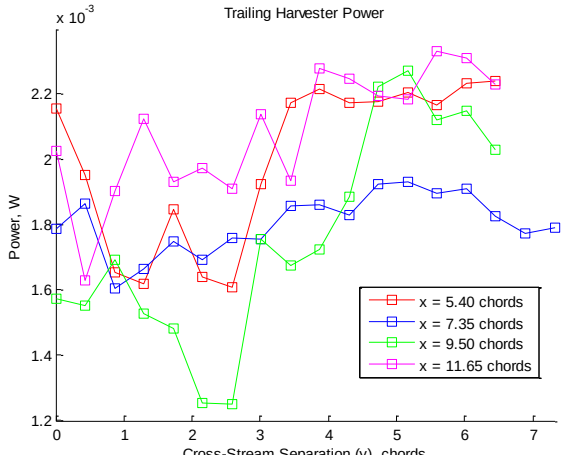

Fig. 10. Trailing Horizontal Harvester Power

5.2 Vertical Harvester Data

Figures 11-14 provide the same plots, only this time for the vertical harvester configuration. Each color line represents a different stream-wise separation, measured in chord lengths, and the plots are functions of cross-stream separation, measured in inches. Figures 11 and 12 provide the frequencies of the leading and trailing harvesters in each position, while Figures 13 and 14 give the power output of the harvesters. The black line in each plot is the base reading for that harvester when it is placed alone in the center of the tunnel test section.

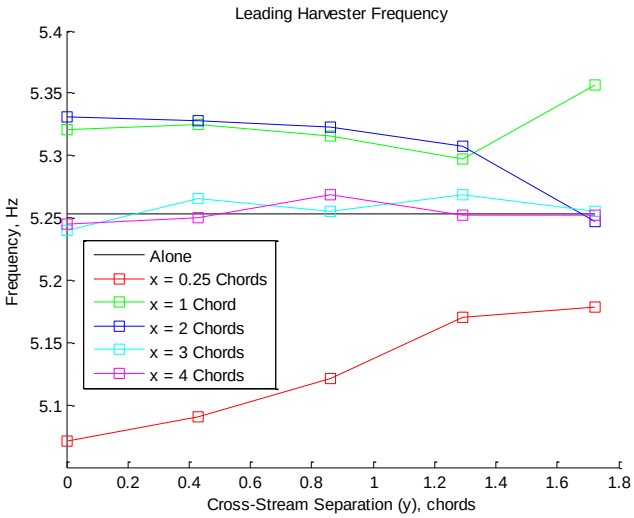

Fig. 11. Leading Vertical Harvester Frequency

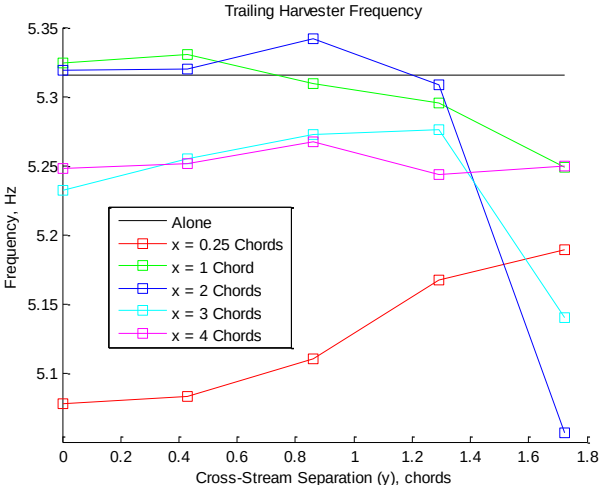

Fig. 12. Trailing Vertical Harvester Frequency

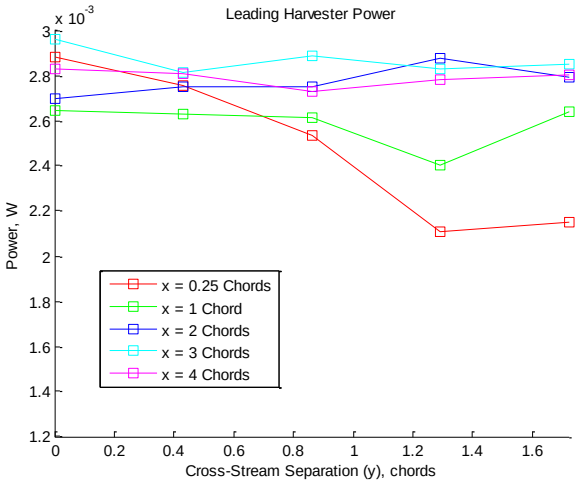

Fig. 13. Leading Vertical Harvester Power

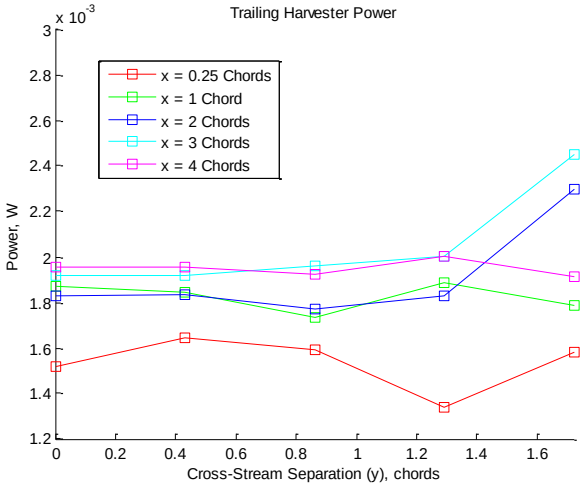

Fig. 14. Trailing Vertical Harvester Power

6 Discussion

6.1 Horizontal Configuration

Overall the frequencies of the horizontal harvesters do not change dramatically, though there are some trends to note. The first stream-wise separation tested with the horizontal harvester was x = 5". We see on the plot of the frequency for the leading harvester that the frequency jumps from a value of approximately 4.90 Hz to 4.98 Hz at a cross-stream separation of 10". This is most likely an aberration, as the frequency stayed at this value through the rest of the x = 5" tests, as well as for x values of 10" and 15". However, there is some significant change in the frequency when the two harvesters were moved close to no stream-wise separation. The frequency drops to about 4.84 Hz at cross-stream separations of 1" and 2", and then steadily rises back up to the steady-state value as the trailing harvester is moved farther to the side. The frequency of the trailing harvester is significantly reduced when there is almost no stream-wise separation between the harvesters. Also, the frequency for other x values drops at a y value of 1". The frequencies then rise back up to a peak and then drop to a minimum between 8-10" cross-stream separation, after which they appear to reach somewhat of a steady value.

The power generated by the leading harvester in the horizontal configuration remains relatively steady for all stream-wise separation except for when x = 0.5". At this separation, the power takes a large dip when y = 3" and then reaches a minimum output at y = 7". It then rises back up to an apparent steady-state level. At the same stream-wise separation, the power of the trailing harvester follows a similar trend, but reaches a minimum at y = 6" instead. The power of the trailing harvester at other stream-wise separations all approximately follow the same trend. However, at each value of x, the minimum power output is at a different position: y = 2", 6", and 1" for the minimums at x = 5", 10", and 15" respectively. It is interesting to note that that largest drop in power, besides that at which the stream-wise separation is minimal, occurs at the largest stream-wise separation tested. After power output reaches a minimum in each case, it then rises back up to reach an approximate stead-state production.

Figure 15 gives the power generation of the two horizontal harvesters at a stream-wise separation of 15". In addition to the data points plotted on previous figures, this plot also includes error bars showing the standard deviations of the ten readings taken at each position. It is obvious that the deviation of the readings becomes smaller after y = 8", corresponding to the locations at which the power generation reaches a stable level. This plot is representative of the other stream-wise separation as well, where the deviation in readings gets smaller when the output begins to reach a steady level. From this trend, it can be inferred that there is significant wake interference affecting the trailing harvester. At a certain critical cross-stream separation, the trailing harvester moves out of the leading harvester's wake and is able to achieve a somewhat stable output level.

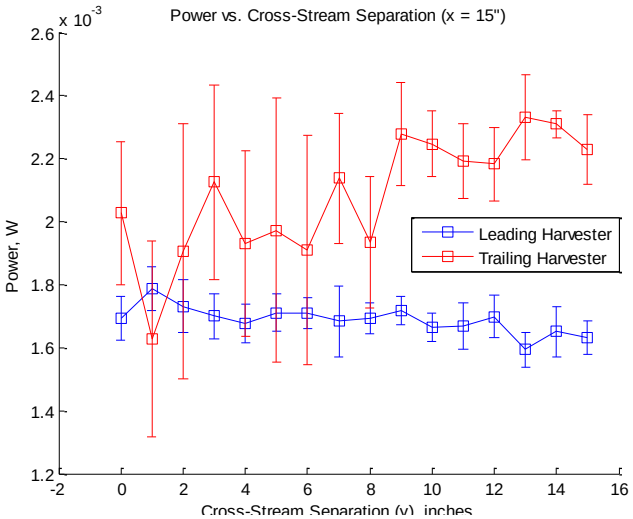

Fig. 15. Horizontal Harvester Power Production at 15" Stream-Wise Separation

6.2 Vertical Configuration

Given that significantly less data has been collected to this point for the vertical configuration, the trends seen in the data are not that revealing. When there is no stream-wise separation between the harvesters, the frequency of the harvesters is much less than the base value, rising steadily as the cross-stream

separation between the two is increased. Otherwise, the frequency of the leading harvester is relatively stable at each stream-wise separation, though it is interesting to note that at x = 1 chord it increases and at x = 2 chords it decreases at the largest cross-stream separation. Similarly, the frequency of the trailing harvester is stable at all other positions, but it drops at y = 4" for x = 1, 2, and 3 chords. The magnitude of this change is largest when the stream-wise separation is 2 chords.

There is a large differentiation in the power produced by the leading harvester when x = 0 chords. The harvester goes from producing about 2.9 mW when y = 0" to producing less than 2.2 mW when y = 3". The trailing harvester produces far less power than at any other stream-wise separation, reaching a minimum of approximately 1.36 mW when y = 3". At x = 1 chords, the leading harvester power takes a dip when y = 3", but is otherwise steady. The output at other values of x for the leading harvester is relatively constant throughout. The power output of the trailing harvester is relatively constant for each value of x, though at 2 and 3 chord length separations the power actually increases somewhat when y = 4".

The trend for the vertical harvester configuration is almost the opposite of what is seen with the horizontal configuration, as is evidenced by Figure 16. Here, the deviation in the readings at each position is relatively small until y = 4". This is indicative of the results at x = 1, 2, and 3 chords, but notably the deviations at both x = 0 and 4 chords remain small at all y positions. It appears the only significant reduction in power for the trailing harvester is when there is no stream-wise separation. Also, at x = 4 chords, there is little to no effect of the wake of the leading harvester on the performance on the trailing harvester. In terms of power production for the leading harvester, the most significant interaction occurs when there is no stream-wise separation. From Figure 12, it would appear that the interference from the trailing harvester is actually constructive at small cross-stream separation, but becomes destructive at y values of 3 and 4 inches.

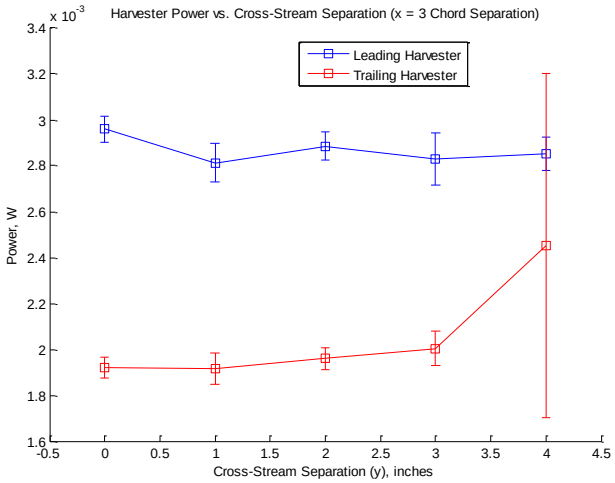

Fig. 16. Vertical Harvester Power Production at x = 3 Stream-Wise Separation

7 Conclusions

Though the steady power outputs of the harvesters fall above and below the base power production lines for different stream-wise separations, it is difficult to draw conclusions considering a majority of this difference is caused by the relative instability of the flow speed in the wind tunnel. However, there are some observations that can give an elementary understanding of some of the interactions. The trailing harvester in the horizontal configuration produces the most power when it is out of the wake of the leading harvester. Momentum is taken out of the flow by the leading harvester in a large swath, measuring 8-11" to the side based on when the trailing harvester reaches steady power production at each stream-wise separation. When the two harvesters are separated by x = 15", it would appear that the flow starts to regain its steady-state momentum as it reaches the trailing harvester. Otherwise, there is obviously some interaction between the harvesters, probably best evidenced by the variation of readings at each position. However, the nature of this interaction cannot be fully understood from this data, making any suggested array formation inconsequential. Therefore, further experimentation is warranted to visually explore the structure of the leading harvester's wake and its flow over the trailing harvester.

The original purpose of the vertical harvester design was to provide clearer understanding of the interaction between multiple harvesters in formation. Again, most of the variation in output is most likely due to the varying conditions in the wind tunnel. A few trends in the data deserve further investigation, specifically the interaction between the harvesters when there is no separation and the power and frequency of oscillation of the trailing harvester at $y = 4$" and beyond. At $x = 0$ chords a substantial change in the leading harvester's power is seen as the cross-stream separation is increased. It is relatively clear that some form of wake is affecting the trailing harvester at $y = 4$", as evidenced by the dropping frequencies at $x = 1$, 2, and 3 chords in Figure 12, the increases in power at $x = 2$ and 3 chords in Figure 14, and the dramatic increase in variation of readings as seen in Figure 16. It is also important to note that any distinguishable form of interaction between the harvesters subsides when the stream-wise separation reaches 4 chords. To make conclusive decisions about the spacing for an array of vertical harvesters, tests should be conducted at larger cross-stream separations to determine the interaction beyond $y = 4$". The interaction between the harvesters when there is no stream-wise separation also needs to be better understood, and possibly confirmed, through further testing. Finally, as with the horizontal configuration, visualization of the flow will provide a more comprehensive understanding of the data.

8 Acknowledgements

This work was supported by Professor Ephrahim Garcia and the Laboratory for Intelligent Machine Systems in the Sibley School of Mechanical & Aerospace Engineering at Cornell University. Wind tunnel experimental capabilities were provided by the Professor Albert George, Chairman of the Master of Engineering Program at Cornell University. Finally, initial concept and previous experimentation, as well as guidance and support through continued experimentation, were provided by Matt Bryant, PhD Candidate in Mechanical Engineering at Cornell University.

References

[1] Anton, Steven.R. and Henry A. Sodano. A Review of Power Harvesting Using Piezoelectric Materials (2003-2006). *Smart Materials and Structures,* 16, 2007.

[2] Robbins, W.P., Morris, D., Marusic, I., and Novak, T. O.. Wind-Generated Electricity Using Flexible Piezoelectric Materials. 17th *IEEE Inernational Symposium on the Applications of Ferroelectrics*, Santa Fe, NM, 2008.

[3] Hodges, Dewey and G. Alvin Pierce. *Introduction to Structural Dynamics and Aeroelasticity*. Cambridge UP, New York, 2002, Chap. 4.

[4] Bryant, Matthew and Ephrahim Garcia. Modeling and Testing of a Novel Aeroelastic Flutter Energy Harvester. *Journal of Vibrations and Acoustics*, in review.

[5] Spedding, G.R. The Wake of a Kestrel (Falco Tinnunculus) in Flapping Flight. *Journal of Experimental Biology*, Vol. 127, pp. 59-78, 1987.

[6] Liao, James C., David N. Beal, George V. Lauder, and Michael S. Triatayllou. Fish Exploiting Vortices Decrease Muscle Activity. *Science*, Vol. 302, No. 5650, pp. 1566-1569, 28 Sept. 2003.

[7] Bryant, M. and Garcia, E. Energy harvesting: a key to wireless sensor nodes. Proceedings of the Second International Conference on Smart Materials and Nanotechnology in Engineering, July 8-11, Weihai, China, 2009.

9 Author Contact Information

Michael Isenberg contact address:

mei7@cornell.edu

Copyright Statement